US DOE, Office of Basic
Energy Sciences

CAMP
Center for Advanced Molecular Photovoltaics
STANFORD UNIVERSITY

Adhesion and Thermomechanical Reliability for PV Devices and Modules

Vitali Brand, Chris Bruner, Fernando Novoa, Jeff Yang *(PhD students)*
Monika Kummel *(Post Doc)*
Reinhold H. Dauskardt (dauskardt@stanford.edu)

Collaborators:

Craig Peters, Roman Gysel and Mike McGehee (Stanford)

Uraib Aboudi and Peter Peumans (Stanford)

David Miller, Michael Kempe and Sarah Kurtz (NREL)

William Hou and Yang Yang (UCLA)

Industry collaborators include Colin Reese, Shawn Scully and Juanita Kurtin (SpectraWatt), Steve Lin (Vitex), Matthew Robinson (Nanosolar), Christine McGuiness and Darin Laird (Plextronics).

Solar Outlook

Then…		*To make a difference…*
1. Efficiency	→	1. Cost
2. Reliability		2. Reliability
3. Cost		3. Efficiency

- Engineer durable solar technologies with robust and predictable lifetimes. Start early in development – avoid roadblocks.
- Leverage from reliability physics in microelectronics – thin-film metrologies, kinetic models, accelerated tests, life prediction.
- Are degradation processes coupled and how?
- Kinetic models for damage evolution - basis for life prediction and accelerated testing (T, environment, stress, solar flux, etc.)
- Effective defensive strategies – e.g. transparent barriers with anti-reflective properties.

Degradation and Reliability of PV Devices and Modules

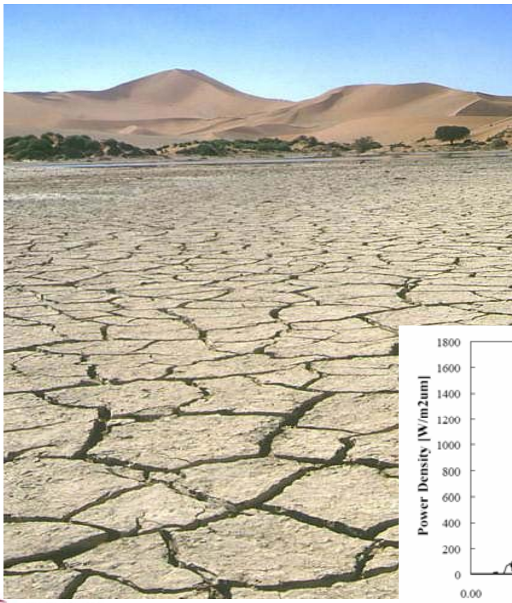

photo from Keele University

Severe operating environments.

Exposure to thermal cycling, stress, moisture, chemically active environmental species, and UV.

Uncertain degradation kinetics and reliability models.

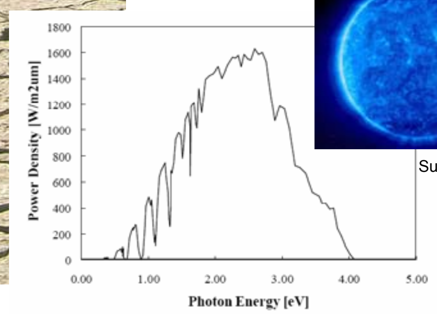

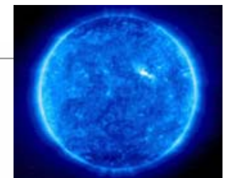

Sun in UV

Solar spectrum from B. Van Zeghbroeck, U. Colorado

STANFORD MATERIALS SCIENCE AND ENGINEERING

Degradation and Reliability of PV Devices and Modules

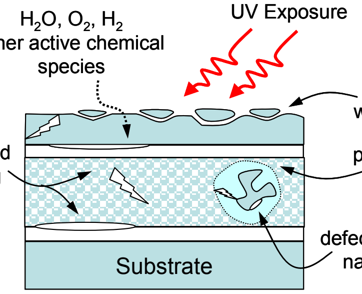

Severe operating environments.

Exposure to thermal cycling, stress, moisture, chemically active environmental species, and UV.

Uncertain degradation kinetics and reliability models.

Activation Energies for Bond Rupture:

VDW ~ 0.001 - .4 eV/bond

H-bonds ~ .1 - .4 eV/bond

Ester Hydrolysis (100% RH)

E* ~ .81 eV/bond

SiO_2 cracking in water

E* ~ 1.39 eV/bond

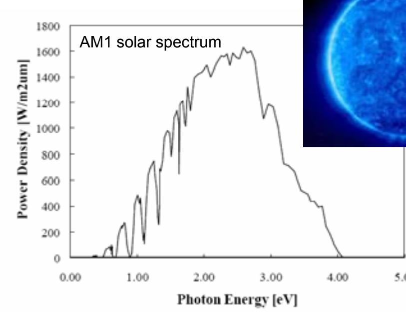

Sun in UV

Solar spectrum from B. Van Zeghbroeck, U. Colorado

STANFORD MATERIALS SCIENCE AND ENGINEERING

Mechanics of Damage Evolution

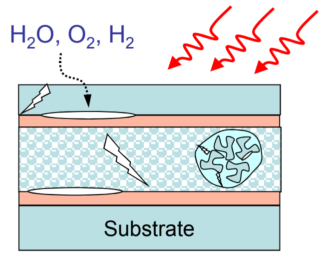

Damage occurs when…

$$\underbrace{G}_{\text{crack driving "force"}} \geq \underbrace{G_c \left[J/m^2\right]}_{\text{cracking "resistance"}}$$

• Lower thin-film stresses – driving force for cracking $G = \dfrac{Z\sigma_f^2 h_f}{\bar{E}_f}$

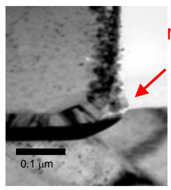

– geometry/structure effects Z

– low modulus organic films

– multiple films, packaging, flexing

• Optimize fracture resistance G_c – cohesion of layers

– adhesion of interfaces

Evolution of Defects and Device Reliability

absence of chemically active environmental species, damage propagates if

$$G \geq G_c \left[J/m^2\right]$$

presence of chemical species and photons, damage propagates even if

$$G < G_c \left[J/m^2\right]$$

environment and stress accelerates defect evolution

Role of coupled kinetic parameters:

- *mechanical stress*
- *temperature*
- *environmental species*
- *photons (photochemical reactions)*

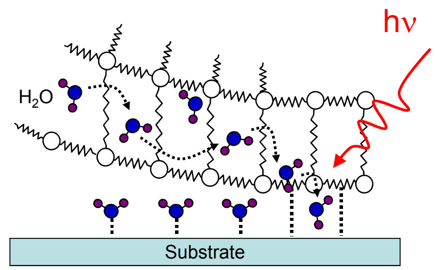

STANFORD MATERIALS SCIENCE AND ENGINEERING

Quantitative Adhesion/Cohesion and Debond Kinetics

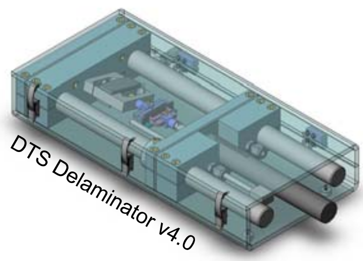

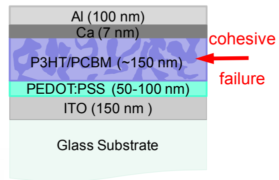

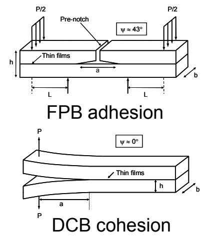

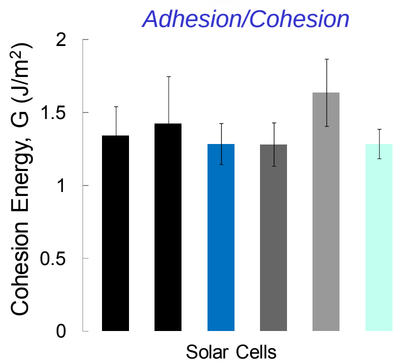

System and support dauskardt@stanford.edu

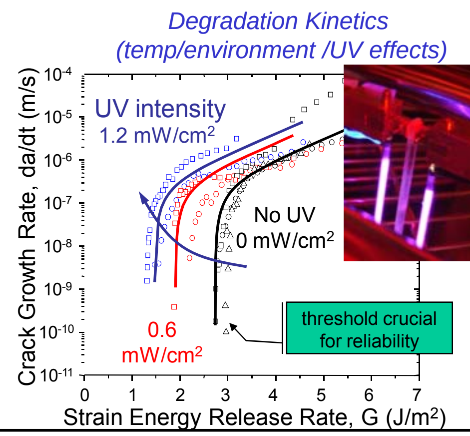

Inherent
Solar Cell Thermomechanical Reliability, G_c

Grad students: Vitali Brand, Jeff Yang and Chris Bruner

Adhesion/Cohesion Sample Preparation

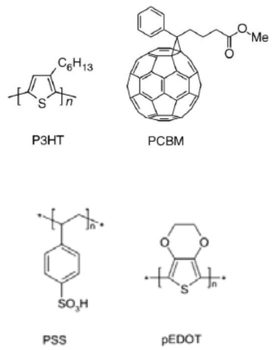

Gunes, et. Al. *Chem. Rev.* 2007.

Thin films sandwiched between elastic substrates

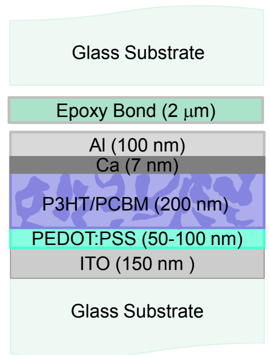

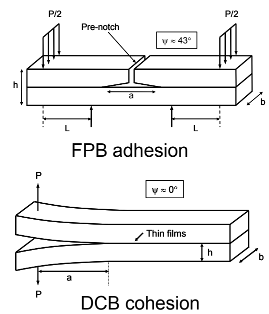

Fabricated 4-point bend adhesion and DCB cohesion test structures using standard epoxy bonding techniques.

Similar transparent glass substrates on each side.

STANFORD MATERIALS SCIENCE AND ENGINEERING

Adhesion/Cohesion of P3HT/PCBM Structures

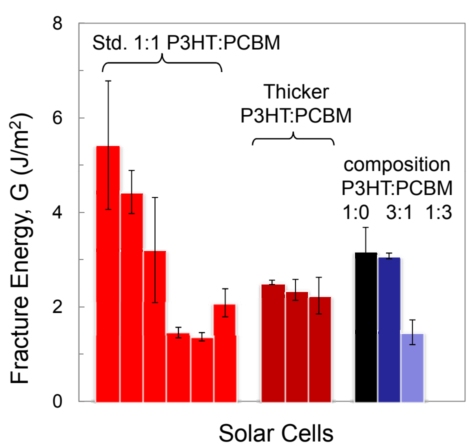

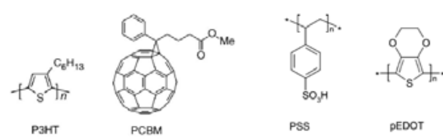

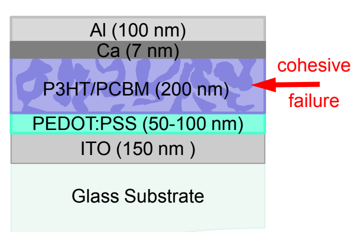

- XPS reveals similar debond path for DCB and 4-pt bend samples
- C ~ 92%, S ~ 6%, O ~ 2%
- Suggests cohesive failure in PCBM:P3HT layer

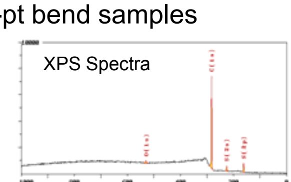

STANFORD MATERIALS SCIENCE AND ENGINEERING

Cohesive Fracture Properties of Dielectrics

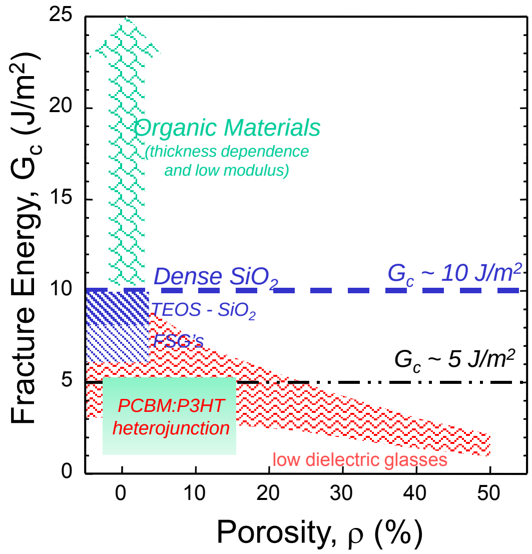

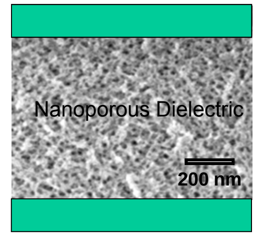

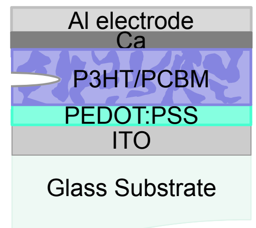

STANFORD
MATERIALS SCIENCE AND ENGINEERING

Factors Effecting Cohesion of P3HT/PCBM Layers

- Heterojunction layer thickness
  - cohesion in polymer layers is sensitive to layer thickness
  - plastic energy dissipation in organic layers

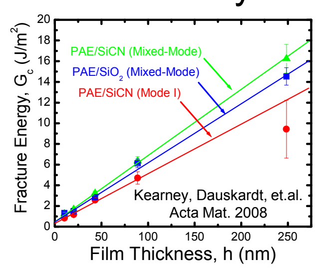

- Composition of the heterojunction layer
  - limited bonding to fullerene – expect low cohesion
  - preliminary measurements indicate higher ratios of P3HT to PCBM make stronger active layer

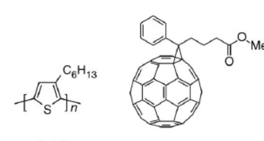

- Annealing
  - morphology of the P3HT:PCBM film changes with annealing, expect effect morphology on cohesion

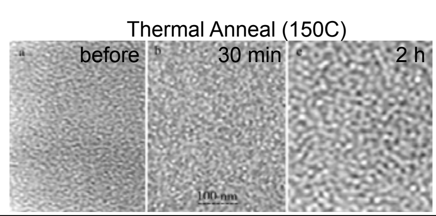

TEM of P3HT:PCBM film
Heeger, et. Al. Adv. Func. Mat. 2005.

STANFORD
MATERIALS SCIENCE AND ENGINEERING

Effect of Thickness of BHJ on Cohesion

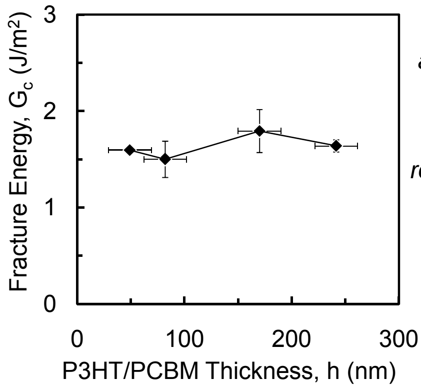

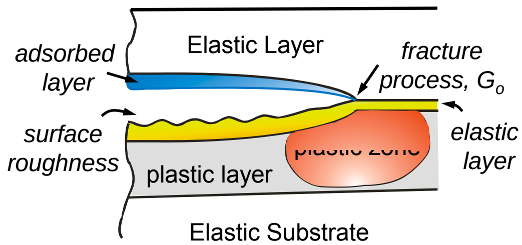

interface chemistry

$$G_{total} = G_o + G_{zone}$$

frictional contact
ductile adjacent layer

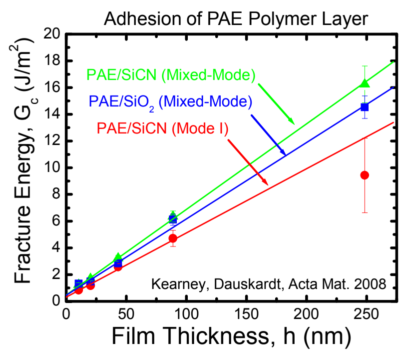

STANFORD
MATERIALS SCIENCE AND ENGINEERING

Effect of Thickness of BHJ on Cohesion

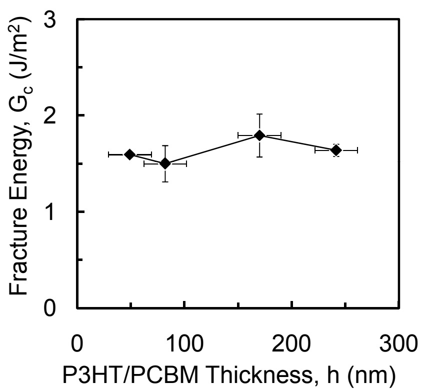

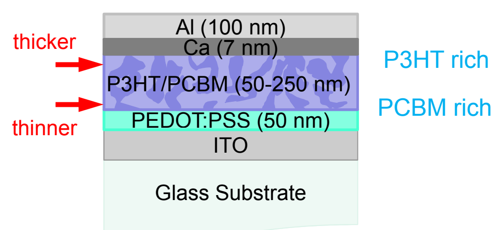

Segregation of PCBM towards bottom PEDOT due to more polar nature of PCBM compared to P3HT

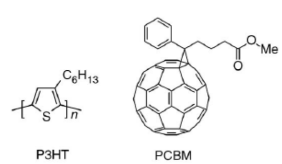

interface chemistry

$$G_{total} = G_o + G_{zone}$$

frictional contact
ductile adjacent layer

STANFORD
MATERIALS SCIENCE AND ENGINEERING

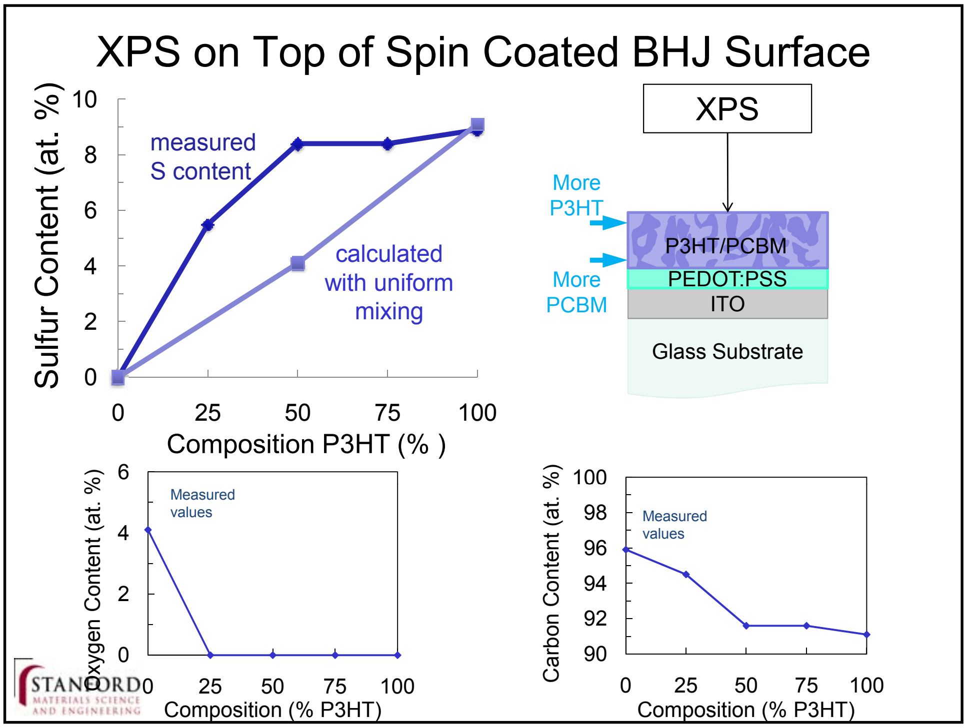
XPS on Top of Spin Coated BHJ Surface
Sulfur Content (at. %)
measured S content
calculated with uniform mixing
Composition P3HT (%)
XPS
More P3HT
More PCBM
P3HT/PCBM
PEDOT:PSS
ITO
Glass Substrate
Oxygen Content (at. %)
Measured values
Composition (% P3HT)
Carbon Content (at. %)
Measured values
Composition (% P3HT)
STANFORD MATERIALS SCIENCE AND ENGINEERING

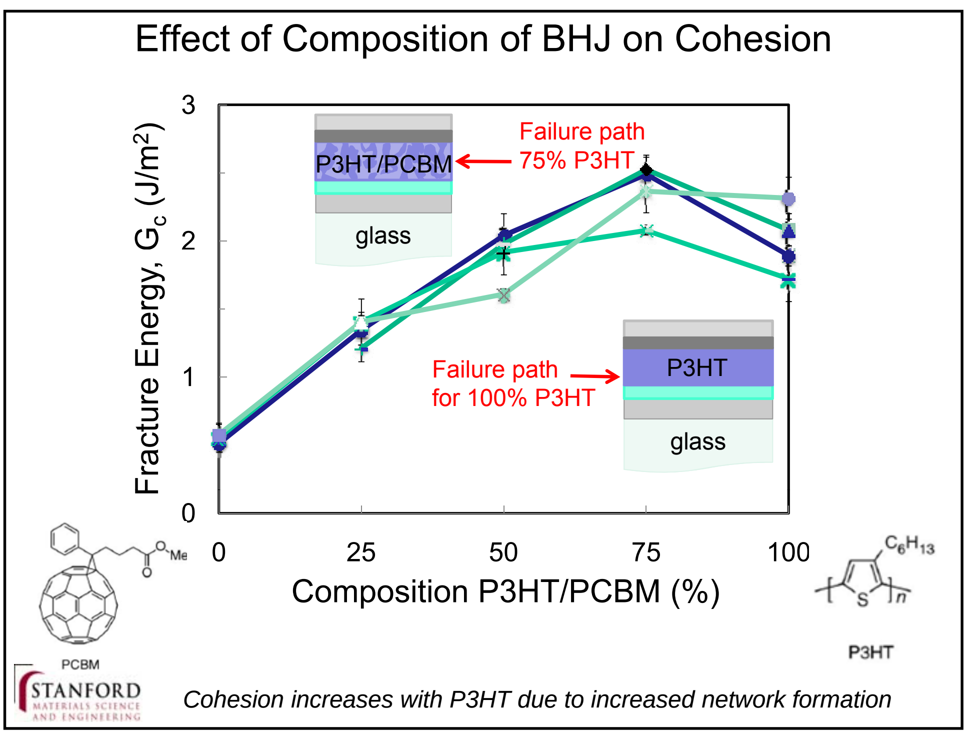
Effect of Composition of BHJ on Cohesion
Fracture Energy, G_c (J/m²)
Failure path 75% P3HT
P3HT/PCBM
glass
Failure path for 100% P3HT
P3HT
glass
Composition P3HT/PCBM (%)
PCBM
P3HT
STANFORD MATERIALS SCIENCE AND ENGINEERING
Cohesion increases with P3HT due to increased network formation

Effect of BHJ Annealing

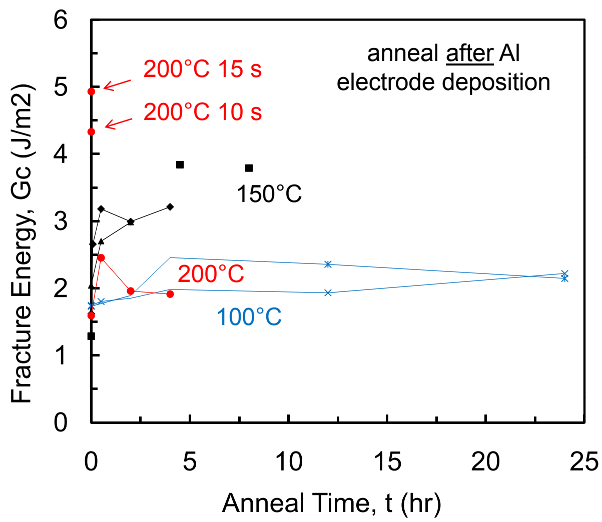

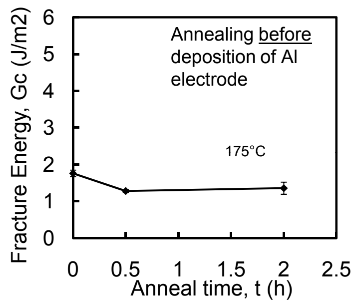

- 150°C anneal increases cohesion significantly
- 200°C anneal degrades the cell
- Anneal before Al deposition does not increase cohesion

STANFORD MATERIALS SCIENCE AND ENGINEERING

AFM of Failure Path Near Ca Interface

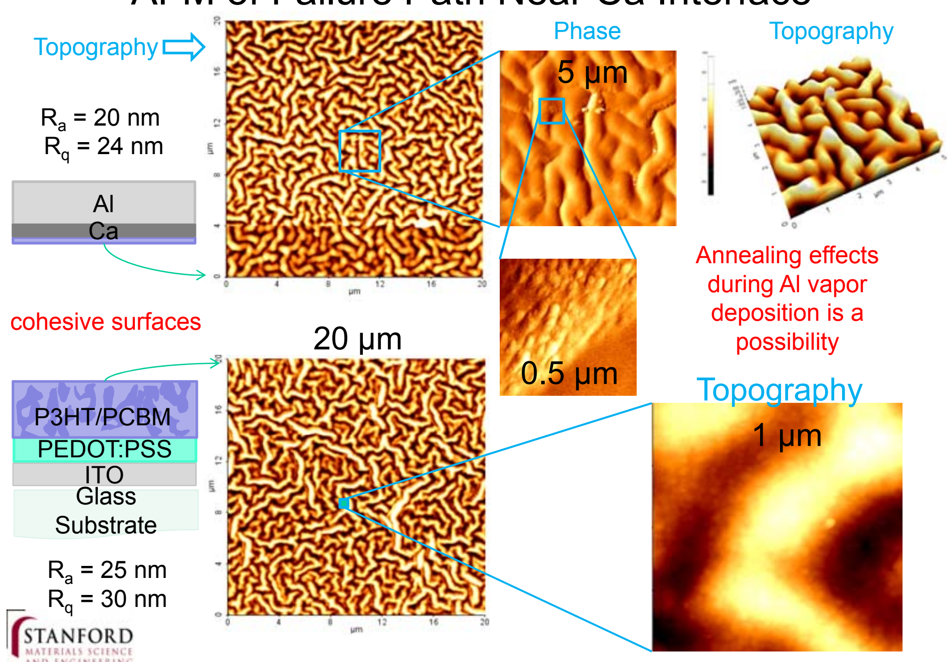

STANFORD MATERIALS SCIENCE AND ENGINEERING

Buckling and Wrinkling in Stressed Films

Lacour et al. Appl. Phys. Lett., Vol. 82, No. 15, 14 April 2003

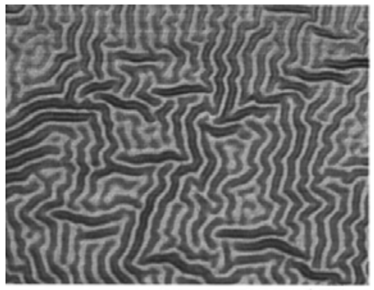

100 µm

Optical image of the wave pattern formed in a 100-nm-thick gold film evaporated on a 1-mm-thick PDMS membrane

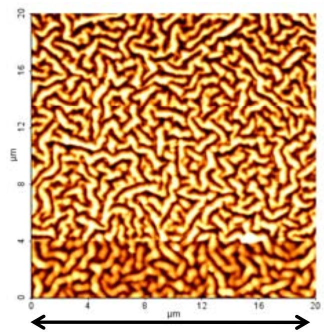

20 µm

Buckling/wrinkling instability at the BHJ/Ca interface resulting from the vapor deposition of Al

STANFORD
MATERIALS SCIENCE AND ENGINEERING

Wrinkling of Stressed Elastic Film on Viscoelastic Layer

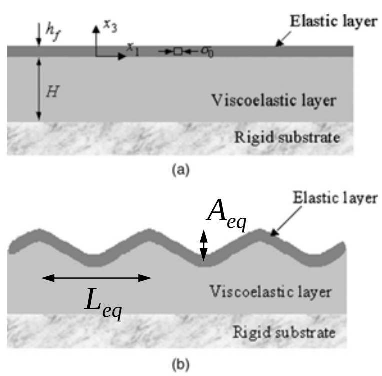

Equilibrium amplitude of sinusoidal wrinkle:

$$A_{eq} = \frac{2\sqrt{1-\nu_f^2}}{k}\left[-\frac{\sigma_0}{E_f} - \frac{(kh_f)^2}{12(1-\nu_f^2)} - \frac{2(1-\nu)}{1-2\nu}\frac{\mu_\infty}{E_f}\frac{1}{k^2Hh_f}\right]^{1/2}$$

Equilibrium wrinkle wavelength: $k=2/L_{eq}$

$$L_{eq} = \pi h_f\left[\frac{2(1-2\nu)}{3(1-\nu)(1-\nu_f^2)}\frac{E_f}{\mu_\infty}\frac{H}{h_f}\right]^{1/4}$$

- *Layers initially flat - elastic layer with* in-plane biaxial compressive stress σ_0.
- Wrinkling to relax stress in elastic layer – viscoelastic layer deforms to maintain conformality.
- μ_∞/E_f is ratio of rubbery modulus of the viscoelastic layer and the elastic modulus of the elastic layer.
- k is the wavevector: $k = 2/L_{eq}$

STANFORD
MATERIALS SCIENCE AND ENGINEERING

Huang et al. Journal of App. Mech. Nov. 2005, Vol. 72

Small Molecule Solar Cell Thin Films

C60

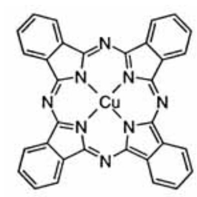

CuPc

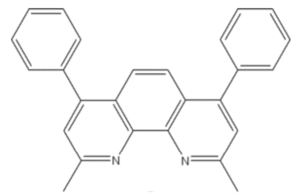

BCP

Ryan Birringer, Uraib Aboudi and Peter Peumans

$$G_c = 1.1 \pm 0.4 \ \ J/m^2$$

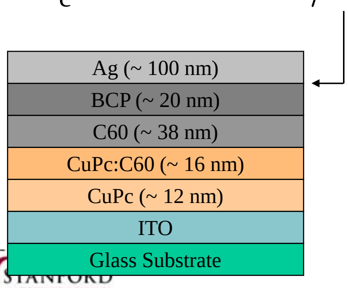

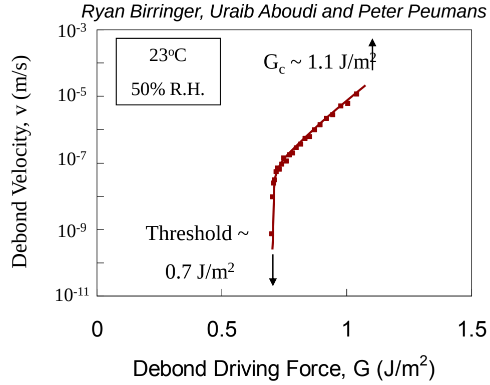

Molecular Bond Rupture Kinetics (Barrier Films)

Grad student: Fernando Novoa and Monika Kummel

$$G \quad < \quad G_c \left[J/m^2 \right]$$

environment and stress <u>accelerates</u> defect evolution

Weathering Test of Polysiloxane Barrier

UV exposure: 28 mW/cm^2 at 6 mm UV-257nm

120 min…………….15 min……………………5 min

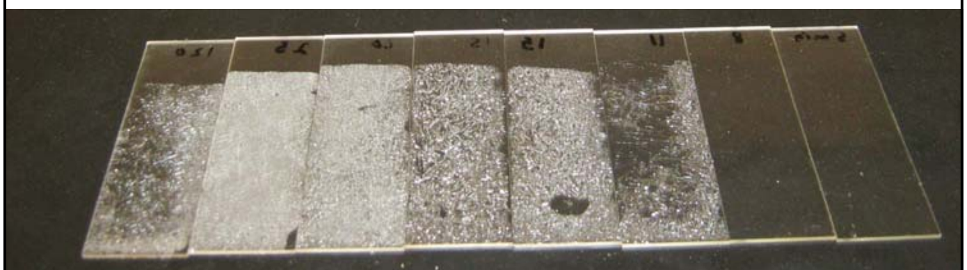

STANFORD MATERIALS SCIENCE AND ENGINEERING

Weathering Test of Polysiloxane Barrier

Film Stress Accumulation with UV Exposure

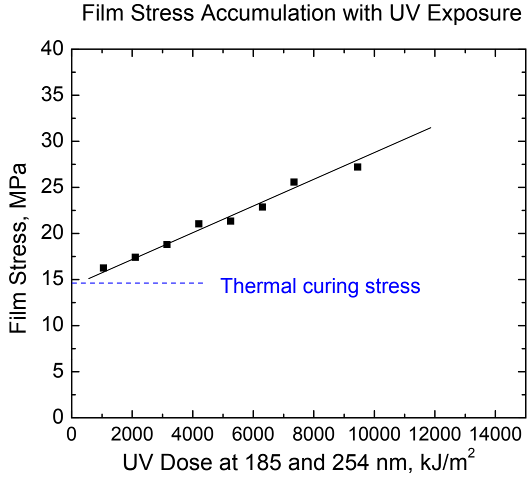

Driving force for damage:

$$G = \frac{Z \sigma_f^2 h_f}{\bar{E}_f}$$

STANFORD MATERIALS SCIENCE AND ENGINEERING

Kamer and Dauskardt - 2009

Environment and Stress Accelerates Damage

Does UV exposure accelerate decohesion in solar cells?

What are the kinetics?

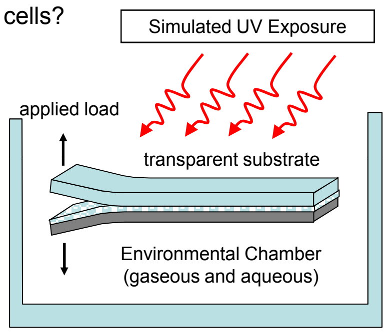

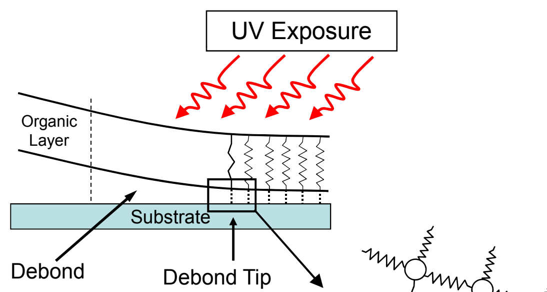

Activation Energies:
VDW ~ 0.001 - .4 eV/bond
H-bonds ~ .1 - .4 eV/bond
Ester Hydrolysis (100% RH)
E* ~ .81 eV/bond
SiO_2 cracking in water
E* ~ 1.39 eV/bond

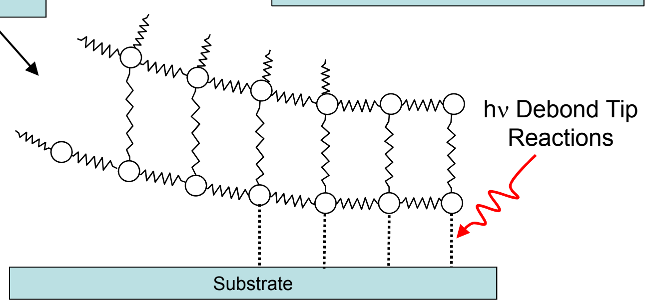

Assessing UV and Environment on Debonding Kinetics

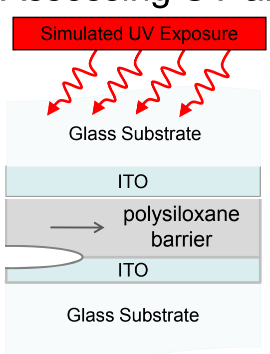

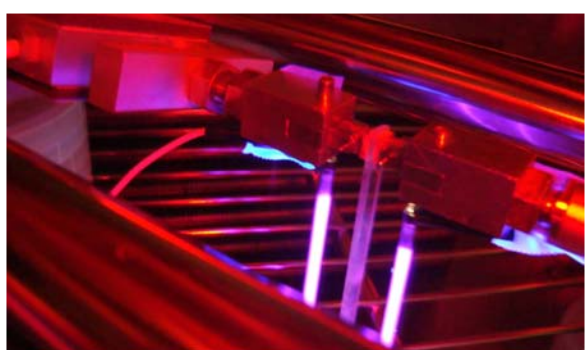

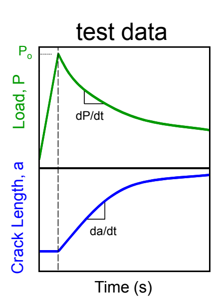

DTS Delaminator v4.0
automated load relaxation debond growth analysis

compliance analysis

sensitivity to < 10^{-10} m/s

Debonding Kinetics

explore role of:

- UV flux
- humidity, O_2, OH, …
- temperature
- mechanical loading

UV Effects on Molecular Bond Rupture

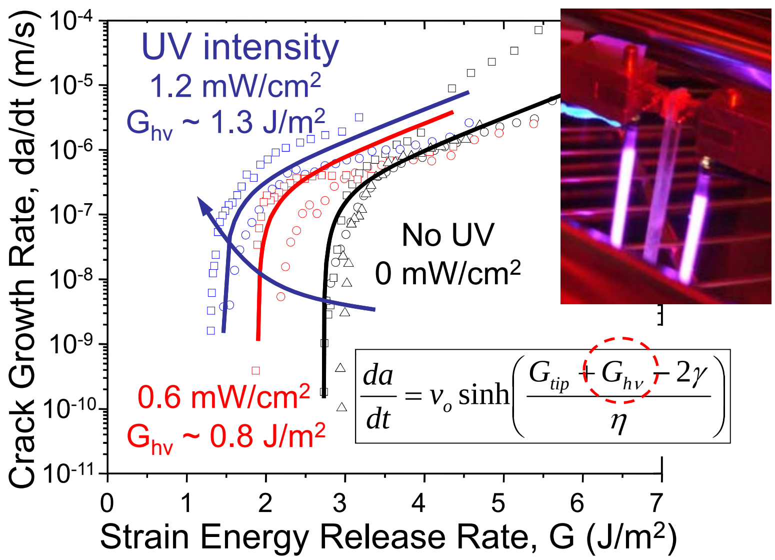

Modeling Bond Rupture Kinetics

- Interaction of moisture with strained debond tip bonds

$$nH_2O + B(\text{debond tip}) \xrightarrow{h\nu} B^*(\text{activated complex})$$

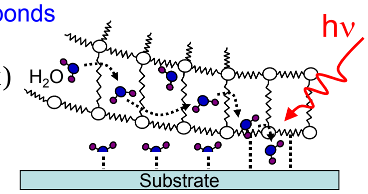

- Atomistic bond rupture models:

$$rate = f_o\left[\exp\left(\frac{-U_+^*}{kT}\right) - \exp\left(\frac{-U_-^*}{kT}\right)\right]$$

- Damage growth rate:

$$\frac{da}{dt} = v_o \sinh\left(\frac{G_{tip} + G_{h\nu} - 2\gamma}{\eta}\right)$$

$$v_o = \frac{2 f_o}{Nw} \exp\left(\frac{-u_1}{kT}\right)$$

Bond Rupture Parameters

N - bonds per unit area
u_o - work of rupture
2γ - N u_o
w - crack width
f_o - attempt frequency
u_1 - energy barrier
η - 2NkT

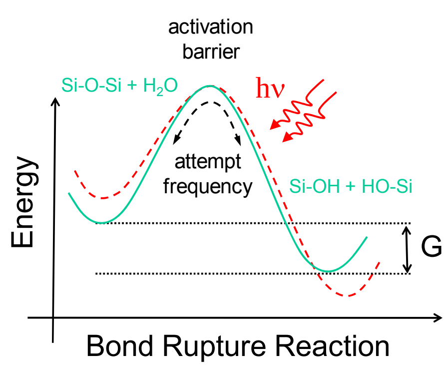

UV Sources

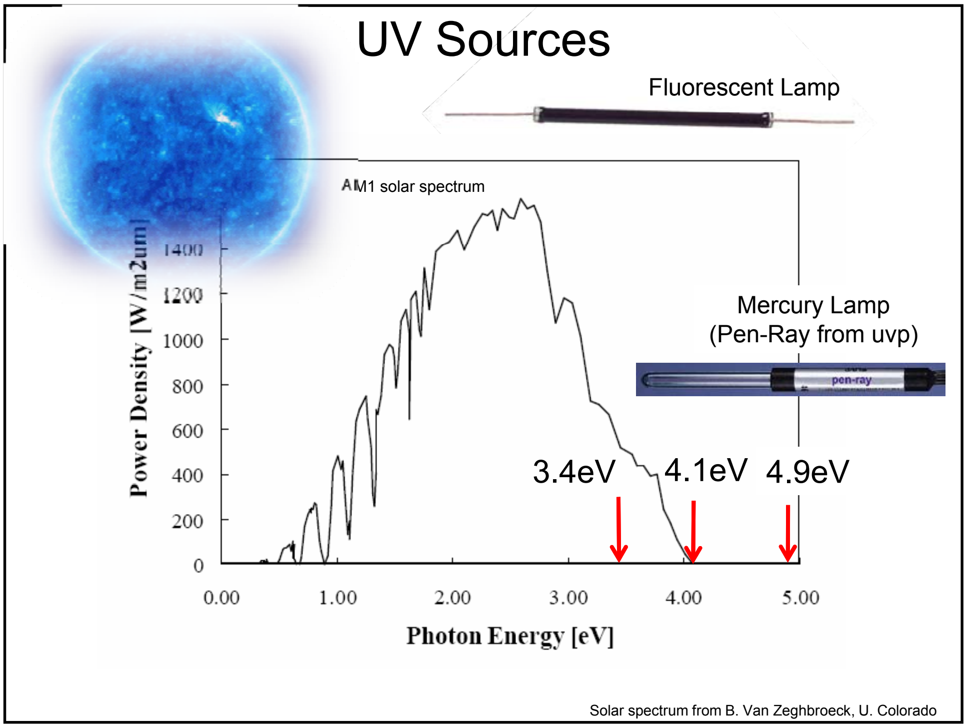

UV Effects on Molecular Bond Rupture

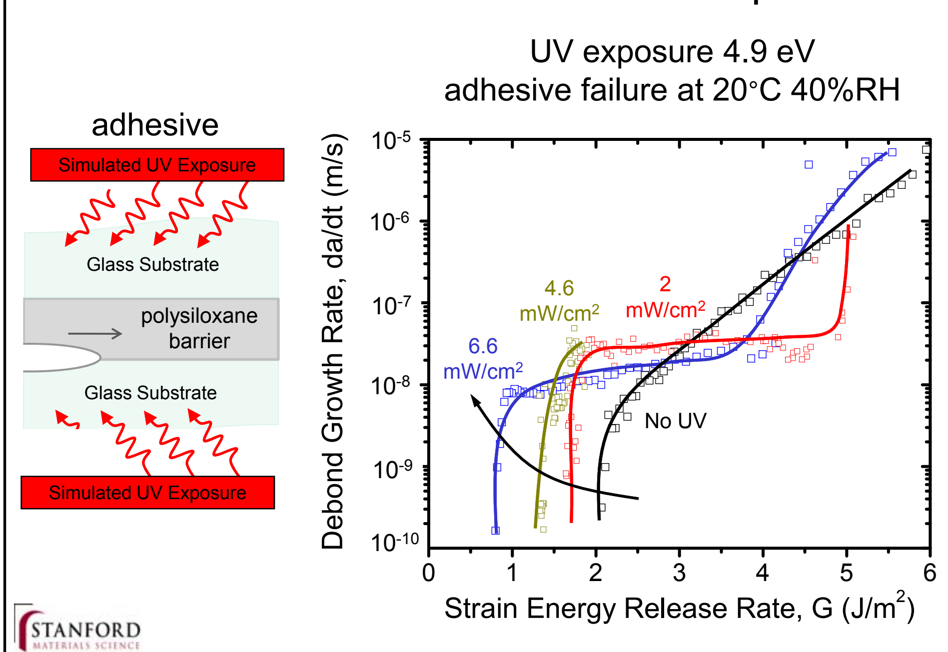

Modeling Bond Rupture Kinetics

- Interaction of moisture with strained debond tip bonds

$$nH_2O + B(\text{debond tip}) \xrightarrow{h\nu} B^*(\text{activated complex})$$

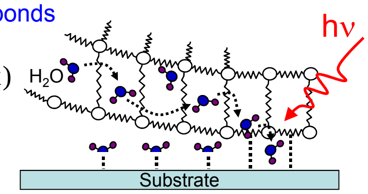

- Atomistic bond rupture models:

$$rate = f_o\left[\exp\left(\frac{-U_+^*}{kT}\right) - \exp\left(\frac{-U_-^*}{kT}\right)\right]$$

- Damage growth rate:

$$\frac{da}{dt} = v_o \sinh\left(\frac{G_{tip} + G_{h\nu} - 2\gamma}{\eta}\right)$$

$$v_o = \frac{2 f_o}{Nw}\exp\left(\frac{-u_1}{kT}\right)$$

Bond Rupture Parameters

N - bonds per unit area
u_o - work of rupture
2γ - N u_o
w - crack width
f_o - attempt frequency
u_1 - energy barrier
η - 2NkT

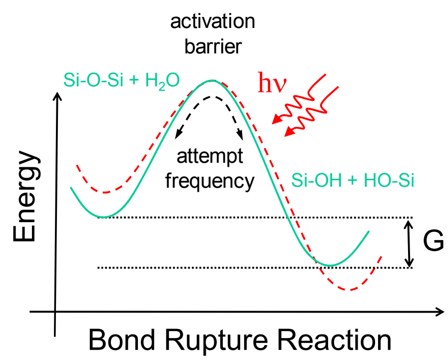

Modeling Bond Rupture Kinetics

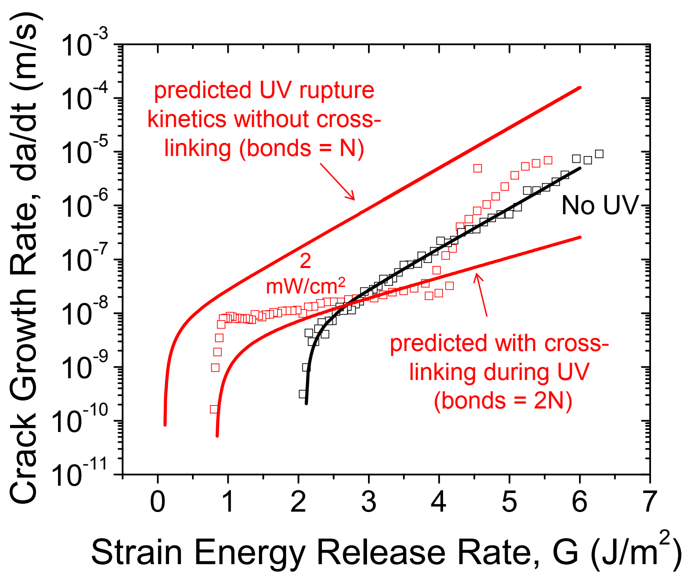

STANFORD MATERIALS SCIENCE AND ENGINEERING

UV Effects on Molecular Bond Rupture

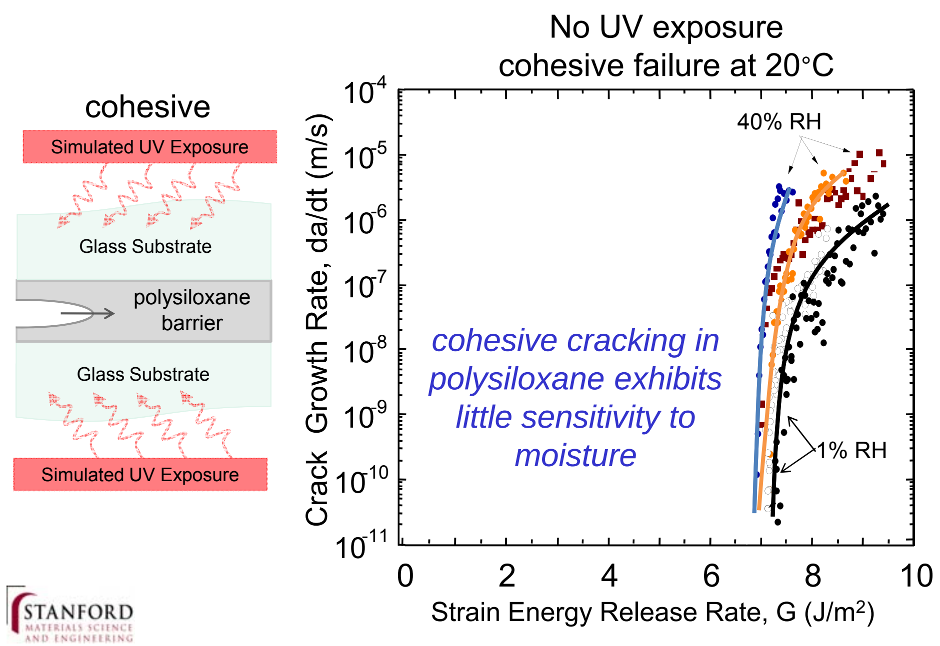

UV Effects on Molecular Bond Rupture

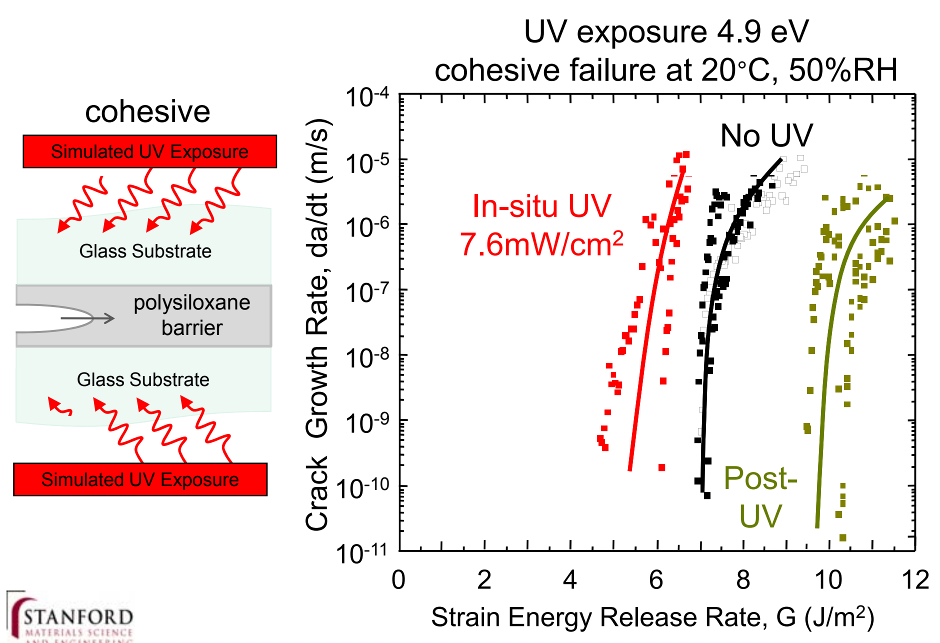

Delamination of EVA-TPE Lamination

- Poly-ethylene vinyl acetate (EVA) copolymer extensively used by solar module manufacturers, particularly for laminating c-Si photovoltaic modules.
- Good optical properties and high adhesive contact with glass cover and Si cells.
- Inexpensive and relatively easy fabrication.

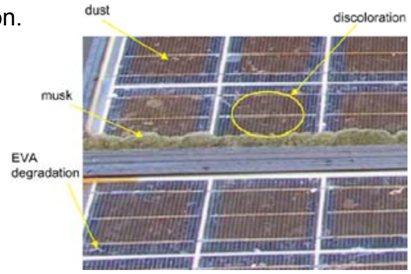

Parreta Antonio, et al., Solar Energy Materials & Solar Cells, 2005

- Delamination can occur between EVA and the front surface of the solar cells.
- More frequent and in hot and humid climates.
- Exposure to atmospheric water and/or ultraviolet radiation leads to EVA decomposition to produce acetic acid, lowering the pH and increasing corrosion.
- EVA Tg ~ -15°C so lower temperatures may result in “ductile-to-brittle” transition in adhesive/cohesive properties.

STANFORD MATERIALS SCIENCE AND ENGINEERING

Delamination of EVA-TPE Lamination

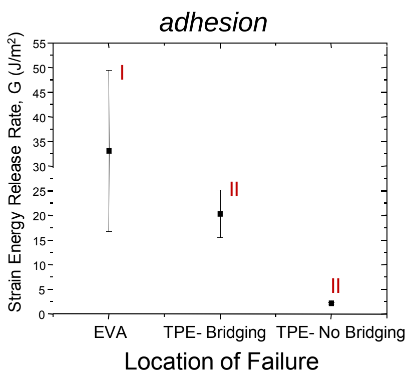

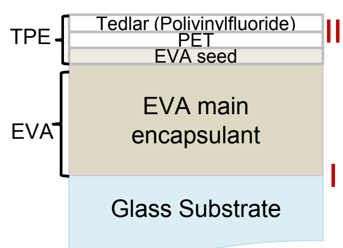

Interface “I” located between EVA and Glass
Interface “II” inside the TPE multilayer

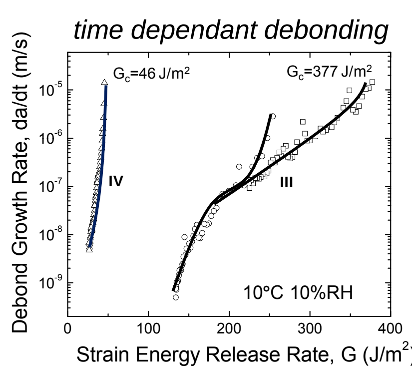

STANFORD MATERIALS SCIENCE AND ENGINEERING

Examples from Microelectronics

Adhesion of Interfaces in Packages:

Role of Functional Group and Surface Coverage

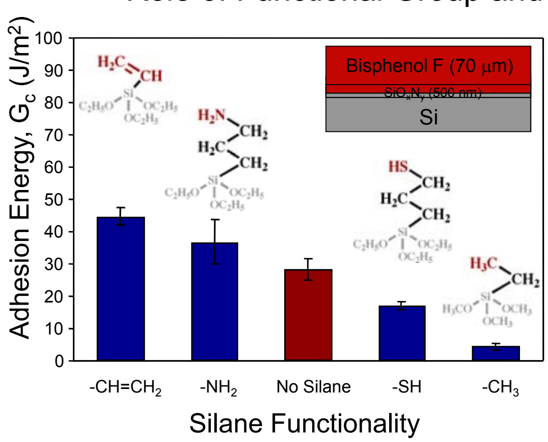

Diglycidyl ether of bisphenol F

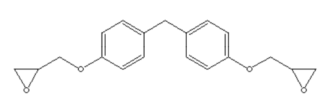

2,4-ethyl methyl imidazole

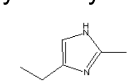

Adhesion energy corrected for surface coverage.

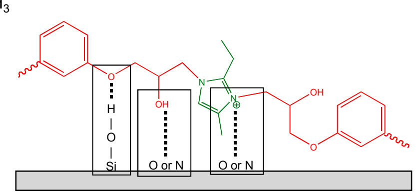

STANFORD MATERIALS SCIENCE AND ENGINEERING

Jenkins, Dauskardt Bravman, J. Adhesion Sci. Tech., 2004.

Adhesion and Debonding in Device Packaging

Anomalous Threshold Behavior

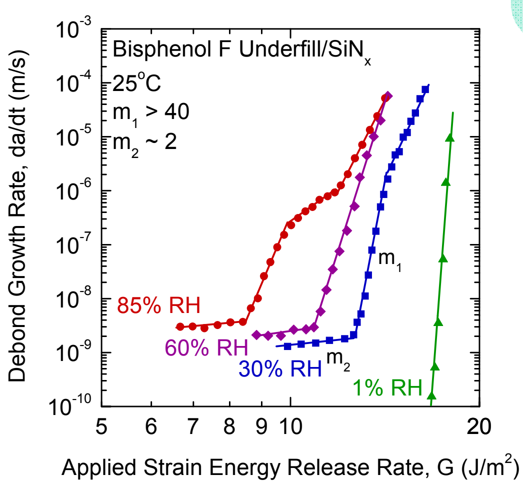

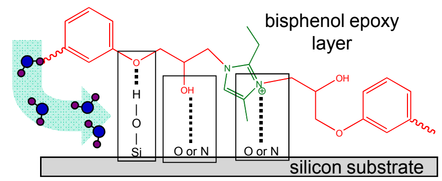

Bulk Na_2O Containing Glasses (Simmons, Freiman, 1981)

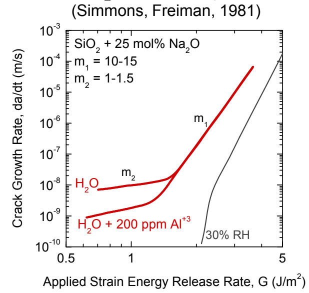

STANFORD MATERIALS SCIENCE AND ENGINEERING

Wang, Sharratt and Dauskardt, Acta Materialia – 2007.

Stress-Dependent Moisture Transport Model

$$D = D_0 \exp(k_2 C + k_3 \sigma) \quad \Leftrightarrow \quad D = D_0 \exp\left(\frac{-E^* + \alpha\sqrt{G}}{RT}\right)$$

Petropolous & Roussis (1978)

$$\frac{da}{dt} = \frac{cux_{H_2O}}{\delta n \Sigma} D_0 \exp\left(\frac{-E^* + \alpha\sqrt{G}}{RT}\right)$$

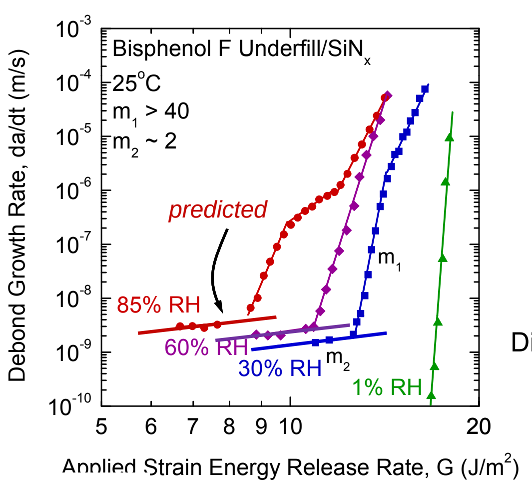

E^* ~ 25 kJ/mol

Diffusion in similar epoxy systems:

DGEBA/1,3-BAC (Barral et al, 1996)	31.2 kJ/mol
TGDDM/DDS (Musto et al, 2002)	34 kJ/mol

Wang, Sharratt and Dauskardt, Acta Materialia – 2007.

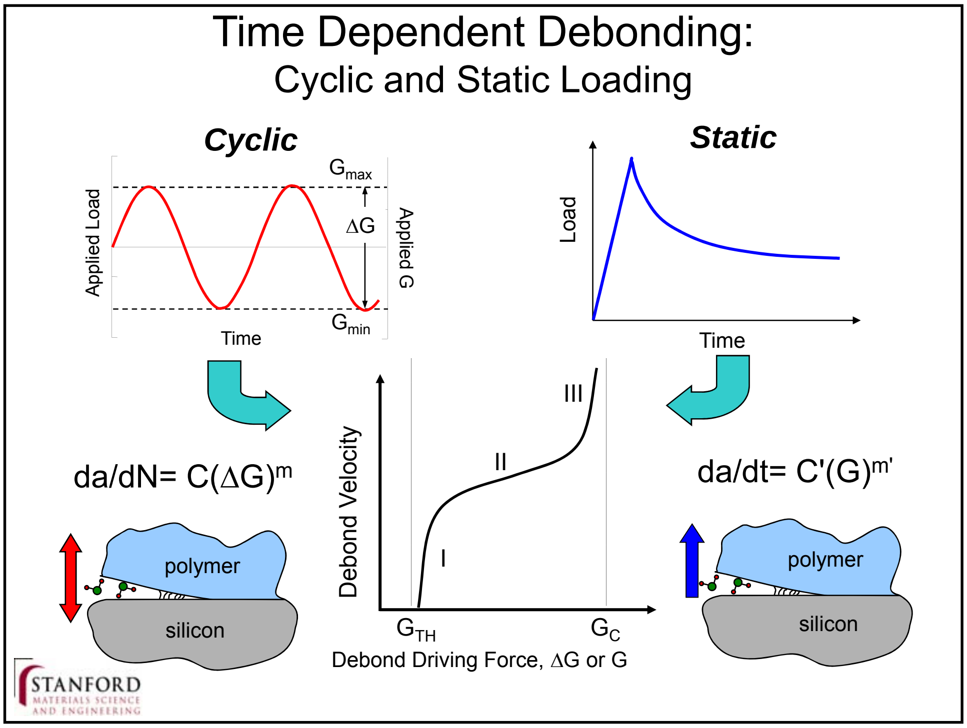
Time Dependent Debonding:
Cyclic and Static Loading
Cyclic
Static
Applied Load
G_{max}
ΔG
Applied G
G_{min}
Time
Load
Time
da/dN= C(ΔG)^m
da/dt= C'(G)$^{m'}$
Debond Velocity
I
II
III
G_{TH}
G_C
Debond Driving Force, ΔG or G
polymer
silicon
polymer
silicon
STANFORD
MATERIALS SCIENCE
AND ENGINEERING

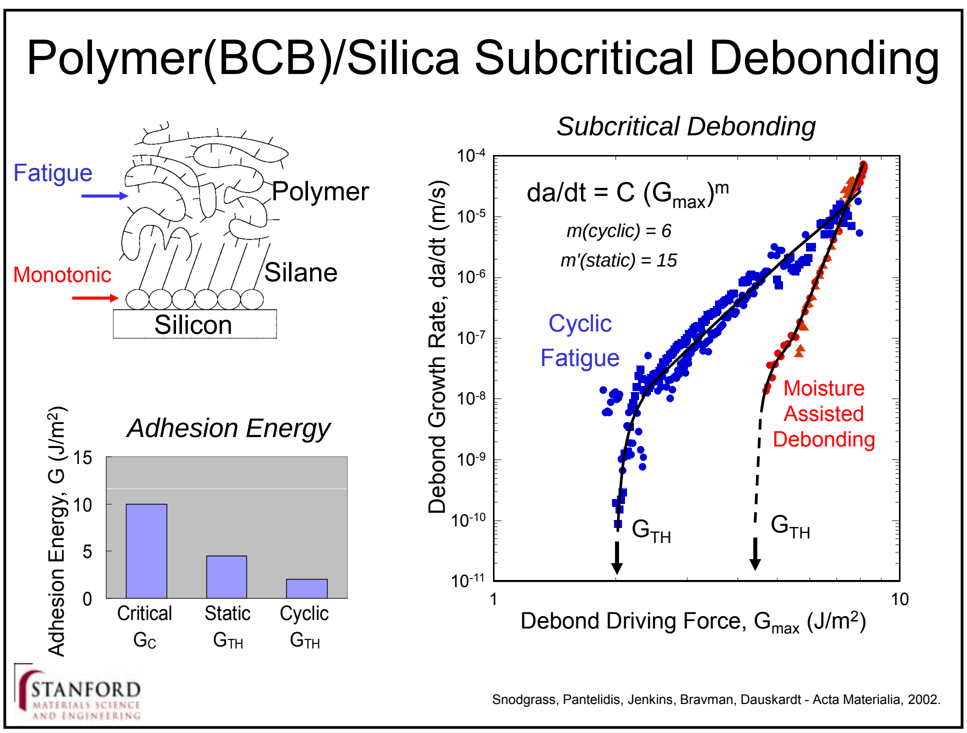
Polymer(BCB)/Silica Subcritical Debonding
Fatigue
Monotonic
Polymer
Silane
Silicon
Adhesion Energy
Adhesion Energy, G (J/m^2)
15
10
5
0
Critical G_C
Static G_{TH}
Cyclic G_{TH}
Subcritical Debonding
da/dt = C (G_{max})^m
m(cyclic) = 6
m'(static) = 15
Cyclic
Fatigue
Moisture
Assisted
Debonding
G_{TH}
G_{TH}
Debond Growth Rate, da/dt (m/s)
10^{-4}
10^{-5}
10^{-6}
10^{-7}
10^{-8}
10^{-9}
10^{-10}
10^{-11}
1
10
Debond Driving Force, G_{max} (J/m^2)
STANFORD
MATERIALS SCIENCE
AND ENGINEERING
Snodgrass, Pantelidis, Jenkins, Bravman, Dauskardt - Acta Materialia, 2002.

Cyclic Stress-Dependent Transport Model

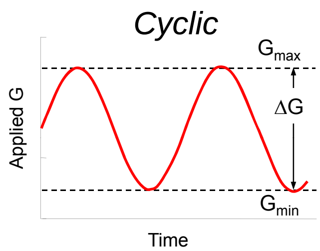

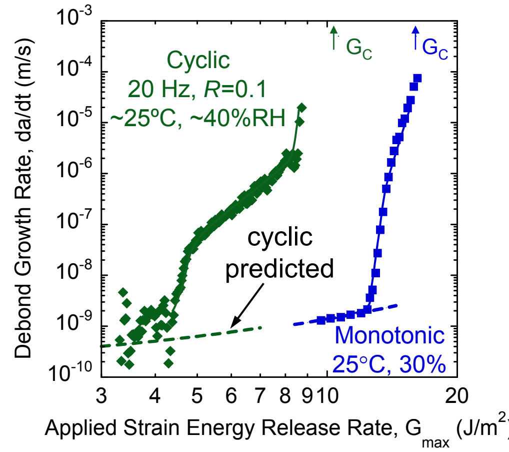

monotonic

$$\frac{da}{dt} = \frac{cua_{H_2O}}{\delta n \Sigma} D_0 \exp\left(\frac{-E_d + \alpha\sqrt{G}}{RT}\right)$$

cyclic (integrate stress-dependent diffusion over fatigue loading cycle)

$$\frac{da}{dt} = \frac{cua_{H_2O}}{\delta n \Sigma} D_0 \exp\left(\frac{-E_d}{RT}\right) g(f,t) \qquad g(f,t) = f\int_0^{1/f} \exp\left[\frac{\alpha}{RT}\sqrt{\left(G_{ave} + \Delta G \sin(2\pi f t)\right)}\right] dt$$

STANFORD MATERIALS SCIENCE AND ENGINEERING

Wang, Sharratt and Dauskardt, Acta Materialia – 2007.

Effect of Fatigue and Thresholds on Package Life

- Significant reduction in life under cyclic loading indicated by arrows.
- Further limits on package life result from anomalous thresholds

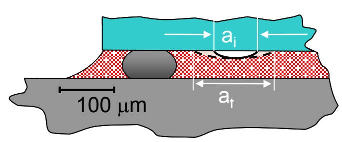

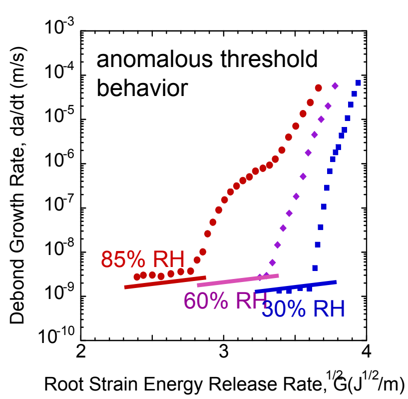

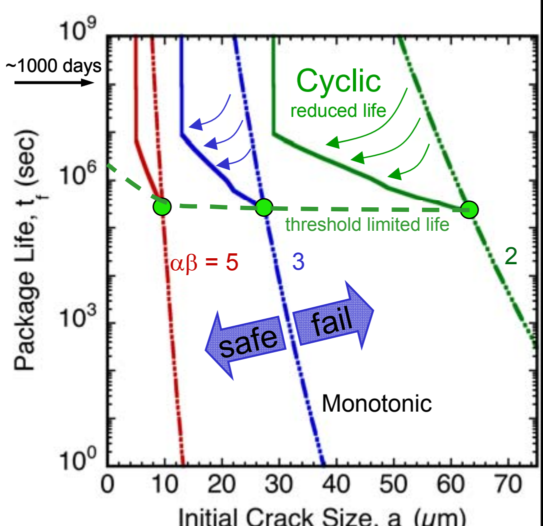

Our Goals for Reliability of PV Technologies

We want to engineer reliable PV devices and modules with robust and predictable lifetimes.

- Leverage from reliability physics in microelectronics – mechanisms, kinetic models, accelerated tests and life prediction
- Develop metrologies to quantitatively characterize thermo-mechanical properties (e.g. adhesion, cohesion), photochemical and environmental degradation processes
- Are degradation processes coupled and how?
- Kinetic models of damage evolution - basis for life prediction and accelerated testing (effect of operating temperature, environment, mechanical stress, solar flux, etc.)
- Effective transparent barriers with anti-reflective properties and low cost.